УДК 539.12.01

SIMULATION OF K^+K^--PAIR PRODUCTION AND DETECTION IN ALICE EXPERIMENT

***B.V.Batyunya, N.V.Slavin, G.Paić**

Simulation of K^+K^--pair production and detection in ALICE experiment for Pb-Pb interactions at LHC energy has been done. The possibility of ϕ meson signal selection over a combinatorial background is demonstrated using the realistic PID efficiencies of ALICE.

The investigation has been performed at the Laboratory of High Energies, JINR.

Моделирование рождения и детектирования K^+K^--пар в эксперименте ALICE

Б.В.Батюня, Н.В.Славин, Г.Пайч

Выполнено моделирование рождения и детектирования K^+K^--пар в эксперименте ALICE для Pb-Pb взаимодействий при энергии LHC. Продемонстрирована возможность выделения сигнала ϕ-мезона над комбинаторным фоном с использованием реалистичных PID-эффективностей в эксперименте ALICE.

Работа выполнена в Лаборатории высоких энергий ОИЯИ.

1. Introduction

The measurement of the yield of the $\phi(s\bar{s})$ sets more stringent constraints on the origin of the observed flavour composition than the K/π ratio. Shifts of the ϕ-meson mass and changes in its line-shape in a hot hadronic medium have been predicted [1]. The production rate and the partial decay width into kaons may change as a consequence of partial chiral symmetry restoration [2]. The ϕ decay will be observed in ALICE both in lepton and kaon channels, and the ratio of these channels might be very sensitive to changes in parton or kaon masses.

We have done the preliminary simulation of the expected experimental mass spectrum of K^+K^- pairs (see Section 11.4.3 in [3]). In this report we present new results with the additional details of the detector simulation particularly for the particle identification possibility.

---

*CERN, Geneva, Switzerland, European Organization for Nuclear Research

2. Physics Generator

The simulations were performed using the SHAKER event generator [4], which includes a direct K^+K^- production and a number of particle decays relevant to the charged kaon analysis, namely the decay channels to charged kaons of ϕ, K^{*+}/K^{*-}, $K^{*0}/\overline{K}^{*0}$ and charm particles. According to the different model prediction for Pb-Pb events at LHC energy (see Section 11.2 of [3]) a flat rapidity distribution was assumed for all particles in the region of $-1 \leq y \leq 1$. To obtain the expected transvers momentum (p_t) distributions, the standard SHAKER method (by m_t-scaling) has been used for ϕ meson. The rates and p_t spectra of K^* resonances have been taken from HIJING model [5]. For charm particles we used results of the model developed for the dimuon spectrometer (see Chapter 6 of [3]), i.e., PYTHIA and JETSET for production and fragmentation and recent cross section calculations [6] scaled from pp collisions with $A^2/2$ (the factor two accounts for nuclear effects such as shadowing).

3. Detector Simulation

The detector response is parametrized in terms of tracking efficiency, particle identification (PID) efficiency and rejection of other (not kaon) charged particles. For tracking efficiency, we used the recent results [7] of track finding and reconstruction with Kalman filter method for the ITS and TPC tracking systems of ALICE set-up. We put the tracking efficiency of 90 % above $p_t = 550$ MeV/c and the efficiency decreasing to 80 % at $p_t = 150$ MeV/c and to 60 % at $p_t = 50$ MeV/c. We included also the transverse momentum dependence of the momentum and angle resolutions as presented in ALICE TP (Figs.11.9 and 11.11 in [3]) obtained with due account of measurement errors, multiple scattering and energy loss. The p_t resolution (for charged kaons) isn't more than 2 % in the p_t region between 0.3 and 4.0 GeV/c and strongly increases at $p_t \geq 0.3$ GeV/c (up to 10 % at $p_t = 100$ MeV/c). The angle resolutions are less than 2 mrad at $p_t > 0.1$ GeV/c (0.15 GeV/c) for $\phi(\theta)$ angle and strongly increase at smaller momentum (up to 5 mrad at $p_t = 50$ MeV/c).

For particle identification information about dE/dx and time-of-flight for kaons, pions, and protons (antiprotons) has been used from the TPC and TOF system, respectively. We don't use dE/dx from the ITS because of the selected momentum (see Section 4). In the process of particle identification we first eliminated the tracks that do not reach neither the TOF at a radius of 350 cm nor the radius of 220 cm in the TPC, because of decay, energy loss or curling. The information about the two last effects has been obtained from GEANT simulation. Further, «fake» kaons (misidentified π^+/π^- and $p/\overline{p}$) were generated by generation of π^+/π^- and $p/\overline{p}$ at $p \geq 350$ MeV/c (because of the momentum cut, see Section 4). It should be noted that about 100 % of pions and $p/\overline{p}$ reach the TOF at this momentum with exception of some pions decaying before. The rejection factor for each π^+/π^- and $p/\overline{p}$ and the PID efficiency for kaons were calculated assuming a time-of-flight resolution of 100 ps and a dE/dx resolution of 7 % (see Section 11.4.1 in [3]). We chose the following lower momentum limit for the PID procedure:

- 1.65 GeV/c for π^+/π^- in the TOF

- 2.7 GeV/c for $p/\bar{p}$ in the TOF
- 0.57 GeV/c for π^+/π^- in the TPC

The rejection factor is about 1,000 (with 95 % PID efficiency for kaons) and the contamination (ratio of the «fake» kaons to the real kaons) is nearly 1 % at these momentum values. The rejection factors were taken as weights of the «fake» kaons in the analysis. To take into account the geometrical inefficiency of the TOF and multiple hits in the counters, we used a special function (momentum dependent) obtained for charged kaons with due account of the matching procedure from TPC to TOF system [8]. Thus, the combined efficiency for kaons (the weight in the next analysis) is a product of the efficiency calculated from this function and of the PID one (determined by the time-of-flight resolution).

4. Results

2.5×10^5 SHAKER events were generated for the analysis with a charged particle rapidity density of $dN_{ch}/dy = 4000$ (some optimistic version) in a rapidity region of $-1 \le y < 1$ and in the polar angle region of $45° \le \theta \le 135°$. The numbers of different primary particles per event are presented in Table 1 (note that $K/\pi = 0.1$ in the standard SHAKER event).

Figure 1 shows the momentum dependences of the kaon finding efficiency and contamination. The kaon finding efficiency is defined as the ratio of identified kaon number

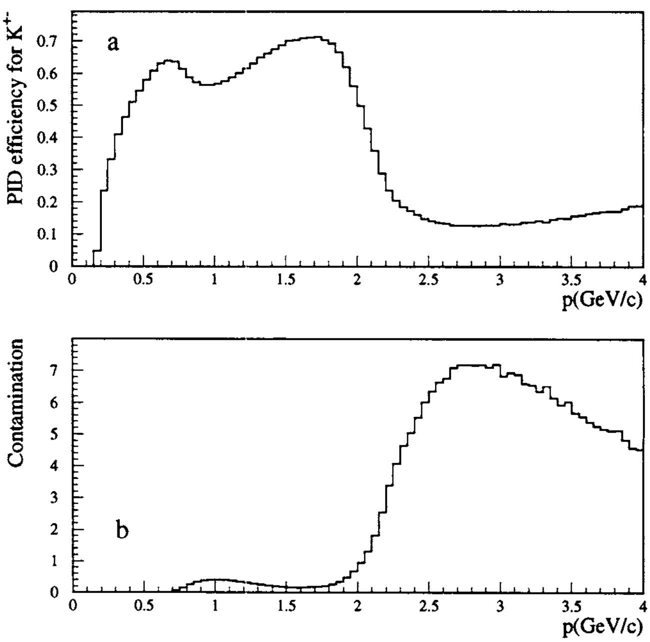

Fig.1. Momentum dependence of kaon finding efficiency (a) and a contamination (b) for the PID efficiency of 95 %

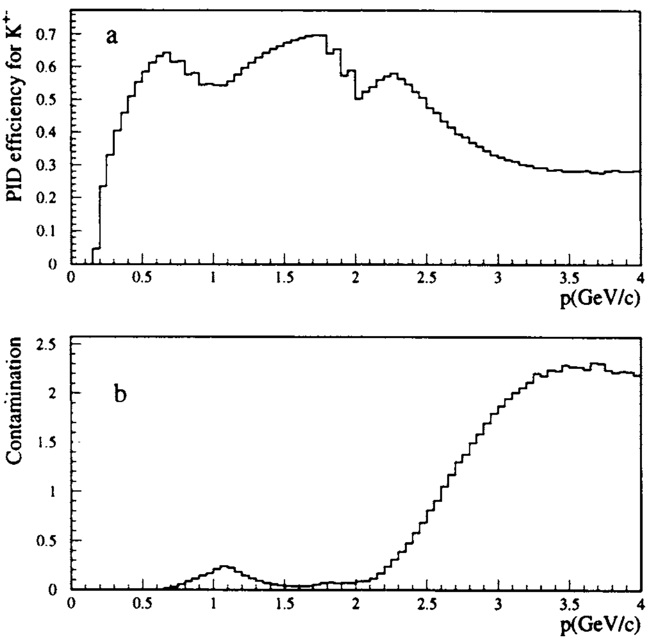

Fig.2. Momentum dependence of kaon finding efficiency (*a*) and a contamination (*b*) for the PID efficiency obtained using the step function (see text)

Table 1. Numbers of different primary particles per event

K^+/K^-	$K^{*0}/\bar{K}^{*0}$	K^{*+}/K^{*-}	ϕ	$c/\bar{c}$
697	50	25	24	14

(the real and «fake» ones) to all generated ones. These dependences have been obtained using the PID efficiency equal to 0.95 (see Section 3). The strong decrease of the full finding efficiency at low momenta is determined by the track curling, kaon decays and energy loss. A reason of the efficiency decreasing at high momenta is the strong rise of the contamination in the TOF region, at $p > 1.65$ GeV/c (see Fig.1*b*). One can see also that the contamination reaches a quite high level (nearly 50 %) in the TPC region ($p \leq 1.65$ GeV/c) as well, and, as a consequence, there is the drop of the efficiency near 1 GeV/c.

To decrease the contamination the following step functions were used for the PID efficiency:

1. For the TPC

PID eff. = 0.95 at $p < 0.7$ GeV/c,
= 0.84 at $0.7 \leq p < 0.8$ GeV/c,
= 0.69 at $0.8 \leq p < 0.9$ GeV/c,
= 0.54 at $p < 0.9$.

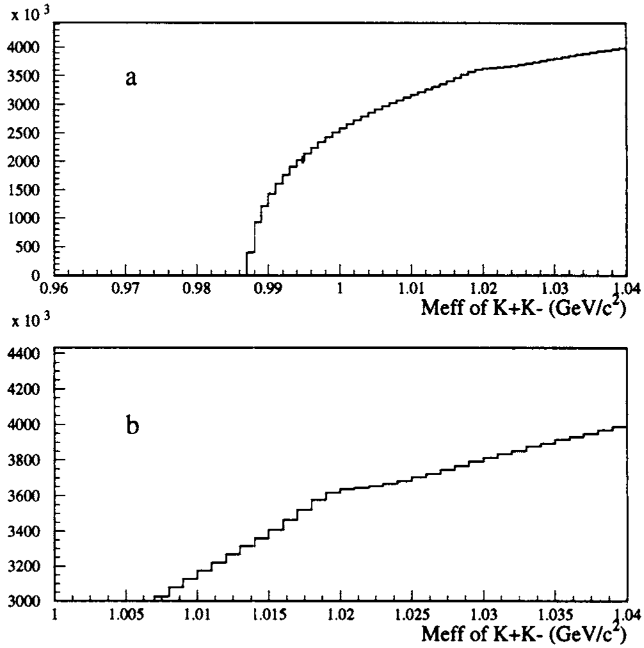

Fig.3. Spectrum of K^+K^- effective mass before any cuts (*a* — full spectrum, *b* — an enlarged view of ϕ resonance)

2. For the TOF
PID eff. = 0.95 at $p < 1.8$ GeV/c,
= 0.84 at $1.8 \leq p < 1.9$ GeV/c,
= 0.69 at $1.9 \leq p < 2.0$ GeV/c,
= 0.54 at $p < 2.0$ GeV/c.

The results are shown in Fig.2. One can see from Fig.2*b* that the contamination does not exceed the level of 20 % both in the TPC and TOF momentum regions at $p < 2.2$ GeV/c (this momentum value was used as a maximal limit in the analysis).

Figure 3*a* shows the K^+K^- effective mass (Meff) spectrum in the acceptance before any cuts. The same spectrum but an enlarged view of ϕ resonance is shown in Fig.3*b*. The ϕ signal is clearly seen over the combinatorial background in Fig.3*b* only and a signal-to-background ratio (S/B) is rather low, $S/B = 0.019$ in the $\pm 2\sigma$ region ($\sigma = 2.4$ MeV/c^2 is the mass resolution).

To improve the S/B level some cuts for different kinematical variables such as p_t of K^+K^- pairs and of individual K^+/K^-, and opening angle between the kaons (see Fig.4) have been studied, and, as a result, a cut $p_t \geq 1.2$ GeV/c for K^+K^- pairs has been chosen. The Meff spectra for kaon pairs passing this cut are shown in Fig.5. Clear ϕ signal is seen in this figure. The curves in Fig.5 are the results of K^+K^- combinatorial background fit by

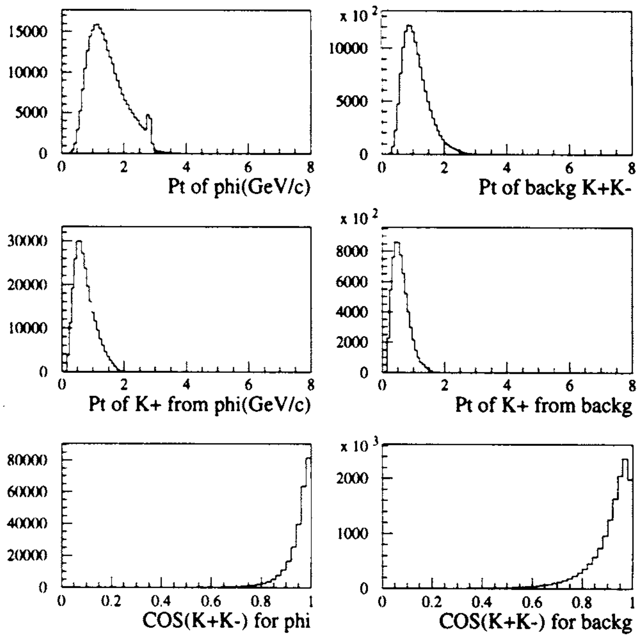

Fig.4. Different kinematical variable distributions for K^+K^- pairs and individual K^+ (see text)

a polynomial function ($p2$) in the Meff region of $1.01 \div 1.03$ GeV/c^2 (the $\chi^2/ndf = 11/17$).

The number of signal event (S) in $\pm 2\sigma$ region around the central mass bin together with the signal-to-background ratio (S/B) and the significance ($S/\sqrt{S+B}$) are shown in Table 2. We note that the significance value corresponds to a 2 % error on the production cross section. We note also that the S/B value is 1.7 times lower at the charged particle density of $dN_{ch}/dy = 8000$ (some pessimistic version).

Figures 6*a* and *b* show the ϕ signal obtained after subtraction of the explicit combinatorial background. The curves are the results of the Breit–Wigner fit (Fig.6*a*) and the Gaussian fit (Fig.6*b*). One can see from these figures that the Breit–Wigner fit is much better than the Gaussian one, meaning that the smearing of the ϕ peak by the momentum resolution does not influence the overall shape of the resonance (the fit results are 1.019 GeV/c^2 and 5.5 MeV/c^2 for mean mass and width of the ϕ signal, respectively). Figures 6*c* and *d* show the same results as Figs.6*a* and *b* (respectively) but after subtraction of the background obtained by the polynomial fit (see Fig.5) (the lines going through the centres of the points have been drawn by hand). The error bars are put as well. The results of the Breit–Wigner fit (Fig.6*c*) are:

Table 2. Signal, signal-to-background ratio and significance for the ϕ in a 2σ region around the central mass bin

$S(\phi)/10^3$	S/B	$S/\sqrt{B+S}$
400	0.036	117

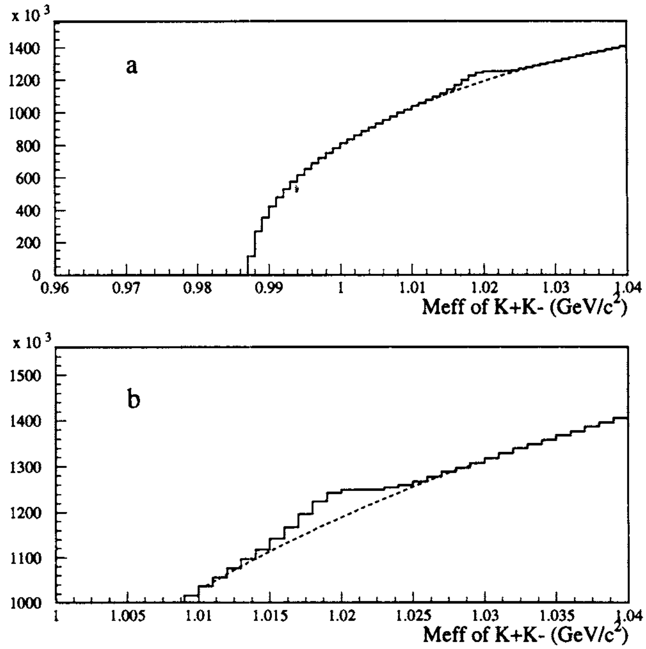

Fig.5. The same spectra as in Fig.3 fit after the cut (see text). The curves are the result of combinatorial background fit by the polynomial ($p2$) function

mean mass is (1.0193 ± 0.0001) GeV/c^2,
width is 4.9 ± 0.3 MeV/c^2,
$\chi^2/ndf = 11/17$.
The ones but for Gaussian fit (Fig.6*d*) are, respectively:
mean mass is (1.0193 ± 0.0002) GeV/c^2,
$\sigma = (2.6 \pm 0.1)$ MeV/c^2,
$\chi^2/ndf = 4/17$.

It is seen that in this case both functions satisfy the distribution and the mass and width are very near to the natural ones. We can suppose, of course, the worse experimental situation because of the known problems with the choice of the combinatorial background, but the accuracy of these measurements in the vicinity of few per cent is seen as quite realistic. One can see also that the Gaussian fit (Fig.6*d*) is somewhat better than the Breit–Wigner one, i.e., the fit result is very sensitive to the background subtraction procedure.

5. Conclusions

The possibility of the ϕ signal detection in ALICE experiment (for Pb-Pb central events at LHC energy) is shown by the simulation. The signal-to-background ratio (S/B) may be increased up to 0.036 and the significance ($S/\sqrt{S+B}$) reachs a value of more than 100

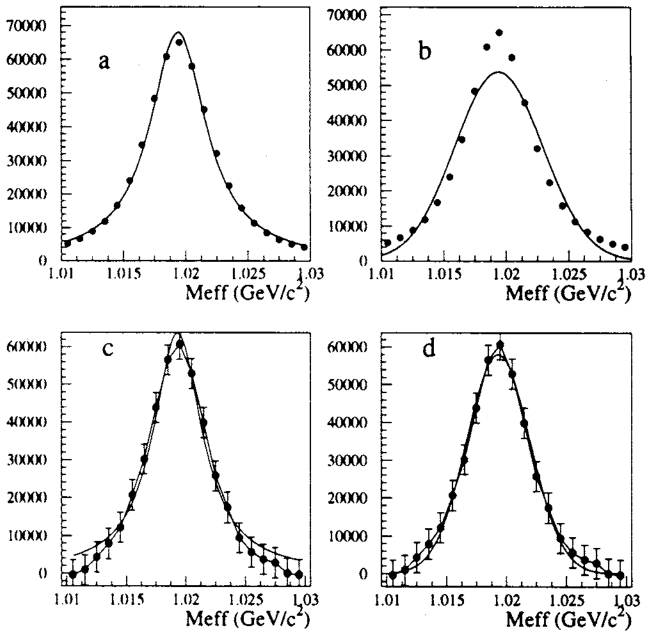

Fig..6. Signal of ϕ meson after substraction of the combinatorial background (*a* and *b* — the explicit background, *c* and *d* — the one obtained by the polynomial fit). The curves are the fit results (*a* and *c* — Breit–Wigner, *b* and *d* — Gaussian)

standard deviations for an amount of 2.5×10^5 events using kinematical cuts. The precisions in the vicinity of few per cent of the ϕ resonance position and width extracted from the fit procedure of the signal shape are seen as quite realistic.

References

1. Asakawa M., Ko C.M. — Nucl. Phys., 1994, v.A572, p.732.
2. Pisarski R.D., Wilczek F. — Phys. Rev., 1984, v.D29, p.338;
   Shuryak E.V. — Nucl. Phys., 1991, v.A525, p.3c.
3. Ahmad N. et al. — «ALICE Technical Proposal», CERN/LHCC/95-71, Geneva, 1995.
4. Antinori F. — Internal Note/SIM ALICE/93-09, 1993.
5. Wang N.X. et al. — Phys. Rev., 1991, v.D44, p.3521; Phys. Rev. Lett., 1992, v.68, p.1480.
6. Gavai R.V. et al. — Preprint GSI-94-76.
7. Batyunya B.V. et al. — Internal Note/SIM ALICE/97-24, 1997.
8. Kiselev S. et al. — Internal Note/SIM ALICE/97-09, 1997.

Received on August 1, 1997.